Case Studies in Construction Materials 17 (2022) e01245

Contents lists available at ScienceDirect

Case Studies in Construction Materials

journal homepage: www.elsevier.com/locate/cscm

Influence of steel fibers and microsilica on the mechanical properties of ultra-high-performance geopolymer concrete (UHP-GPC)

Yazan Issa Abu Aisheh [a], Dawood Sulaiman Atrushi [b], Mahmoud H. Akeed [c,*], Shaker Qaidi [b], Bassam A. Tayeh [d]

[a] Civil Engineering Department, Middle East University, Amman 11831, Jordan
[b] Department of Civil Engineering, College of Engineering, University of Duhok, Duhok, Kurdistan Region, Iraq
[c] School of Civil and Environmental Engineering, University of Technology Sydney (UTS), Sydney, Australia
[d] Civil Engineering Department, faculty of Engineering, Islamic University of Gaza, Gaza Strip, Palestine

ARTICLE INFO

Keywords:
Microsilica
Steel fibers
Ultra-high performance geopolymer concrete
Mechanical characteristics

ABSTRACT

Due to the advantages and challenges specific to geopolymer concrete, especially the ultra-high-performance geopolymer concrete (UHP-GPC) ones, additional studies are warranted. This paper aims to improve the understanding of UHP-GPC by investigating its properties. This research investigates the influence of steel fiber and microsilica (also known as silica fume) on the mechanical characteristics of ultra-high performance geopolymer concrete (UHP-GPC). Three different volume fractions of steel fiber of 0%, 1%, 2%, and 3% and four microsilica volumes by the total mass of the binder of 5%, 10%, 15%, and 25% were utilized. The compressive strength, splitting tensile strength, flexural behavior, and fracture energy are all investigated. Besides, the SEM analyses were performed to understand the mechanism of strength improvement based on the reaction products and micromorphology. The results show that by increasing the amount of microsilica, the amount of steel fiber can be decreased without changing the way UHP-GPC mechanical characteristics.

1. Introduction

Ultra-high-performance concrete (UHPC) is a generic term referring to a composite made of ordinary Portland cement (OPC) that has an ultra-high compressive strength, better durability, and high toughness [1]. It is especially well suited for the construction of blast resistant structural elements [2], long span bridges [3,4], and structures exposed to severely aggressive environments [5,6]. Nonetheless, the mass of OPC in UHPC is typically 750–1200 kg/m^3, which is 2–3 times the amount in conventional concrete; the production of Portland cement requires significant amounts of natural resources and energy and creates significant amounts of carbon dioxide. Producing one ton of clinker is predicted to require 6.7 MJ of energy and emit approximately 0.83 tons of carbon dioxide [7,8]. The researchers attempted to lower the binder volume and substitute extra cement-based materials for OPC. Yu et al. [9] stated that a UHPC matrix with a reduced binder volume of 655 kg/m^3 was made, resulting in a 31% reduction in carbon emissions [10,11].

In comparison to OPC, geopolymer is a low-carbon binder, and clinker-free [12–14]. It is made by activating solid alumino-silicate

* Corresponding author.
E-mail address: mahmoud.akeed@uts.edu.au (M.H. Akeed).

https://doi.org/10.1016/j.cscm.2022.e01245
Received 19 April 2022; Received in revised form 8 June 2022; Accepted 12 June 2022
Available online 15 June 2022

resources like fly ash [15], GBFS [16,17], and metakaolin [18–20] with alkaline solutions like silicate, carbonate, alkali hydroxide, and/or sulfate. It may be used to create geopolymer concrete with mechanical characteristics equal to those of OPC concrete [21–23]. The most recent advancement in sustainability has resulted in the endeavor to make UHP-GPC by employing geopolymer as a binder. Ambily, Ravisankar, Umarani, Dattatreya and Iyer [24] showed that the greatest compressive strength and flexural strength of UHP-GPC with 2% steel fiber were 176 MPa and 14 MPa after 28-days, respectively when activated with hydroxide solutions and alkali silicate. Wetzel and Middendorf [25] and Aydın and Baradan [26] also employed microsilica and GBFS to make UHP-GPC, achieving compressive strength of more than 150 MPa. Numerous publications have indicated that pure GBFS-based GPs exhibit difficulties like rapid setting [27–29], high shrinkage [15,30,31], low flowability [32–34], and mechanical property loss during carbonation [35–37]. Blending GBFS and fly ash appears to be more hopeful than utilizing pure GBFS for obtaining good fresh and hardened characteristics and durability of geopolymer concrete [38–40]. There appears to be considerable space for improvement in these areas of UHP-GPC composition.

The two primary components of UHP-GPC are steel fiber and microsilica. The addition of steel fiber improves impact resistance and ductility substantially [41,42]. Aydın and Baradan [26] showed that when the steel fiber volume was raised to 2%, the addition of steel fibers with a length of 6 and 13 mm had a negligible effect on the compressive strength, flexural strength, and toughness characteristics of UHP-GPC. Moreover, because of the relatively high cost of fiber, proper control of its composition is critical for commercialization and applications [43–45].

Microsilica plays a vital part in strengthening the mechanical and long-term characteristics of OPC-based UHPC, namely throughout its dense packing impact [46–48]. Moreover, a previous study has shown that adding 10–15% microsilica to UHPC improves its rheological characteristics [49–51]. Although numerous prior studies indicated that adding microsilica to geopolymer concrete increased strength development, it decreased workability [52–54]. Wetzel and Middendorf [25] revealed that adding a sufficient amount of microsilica improved the workability and compressive strength of UHP-GPC.

2. Research significance

Due to the advantages and challenges specific to the geopolymer concrete, especially the UHP-GPC ones, additional studies are warranted. This paper aims to improve the understanding of UHP-GPC by investigating its properties.

3. Materials and samples characteristics

The following raw materials are employed to produce UHP-GPC mixtures in this investigation: fly ash, GBFS, and microsilica. Table 1 summarizes the chemical composition of various materials. Fly ash, GBFS, and microsilica have an effective surface area of 290, 455, and 1860 m^2/kg, respectively, with an average particle size of 38, 17, and 0.18 μm, respectively.

An alkaline activator is employed to synthesize UHP-GPC. This activator is prepared using sodium silicate (SiO_2), sodium hydroxide (NaOH), and water that has been allowed to cool to ambient temperature for one day prior to the production of UHP-GPC. To begin, the binders (fly ash, GBFS, and microsilica) were dry blended for 3 min, followed by the addition of silica sand and another 2 min of blending. The activator was then applied to the mixture and blended for 3 min. The industrial-class NaOH in form of pellets is 95% pure. The SiO_2 is a high-quality commercial waterglass composed of 64% water, 28% silicon dioxide, and 6% sodium oxide by mass.

Steel fiber was utilized to make fiber-reinforced concrete, as seen in Fig. 1. Table 2 summarizes the characteristics of steel fiber. Depending on previous studies [15,55,56], this investigation employed a constant water/binder ratio of 0.30. The influence of steel fiber amount on mechanical behavior was investigated by employing an activator with a Na_2O concentration of 6% and a modulus of 1.6, UHP-GPCs with a fly ash/GBFS mass ratio of 1:4, a microsilica dose of 10%, a silica sand/binder ratio of 1:1, and three different steel fiber volume fractions of 1%, 2% and 3%. Moreover, a control (R-0) without steel fibers was developed to better understand the effect of steel fiber content on compressive strength, and modulus of elasticity. Furthermore, to evaluate the influence of microsilica on mechanical characteristics, while maintaining the constant of other factors of the proportions of the mixture, microsilica was blended in four mass ratios of 5%, 10%, 15%, and 25% with a steel fiber volume of 0%. The ratios of the UHP-GPC mixtures are shown in Table 3.

All mixtures were produced at room temperature of 25 °C and relative humidity of 70%. To accomplish this, all ingredients were

Table 1
Chemical components of binder materials.

Chemical component	GBFS	FA	Microsilica
SiO_2	96.44	56.90	35.31
CaO	1.55	1.85	38.51
Al_2O_3	–	31.88	16.56
K_2O	0.73	1.98	0.67
MgO	0.23	0.48	6.88
Na_2O	0.67	2.52	0.32
Fe_2O_3	0.56	2.55	0.57
SO_3	–	0.43	2.57
Others	0.85	–	–
LOI at 1000 °C	–	4.44	1.7

Fig. 1. Steel fiber utilized in this investigation.

Table 2
Properties of steel fiber.

Type	Form	Length (mm)	Dia. (mm)	Aspect ratio	Specific weight (kg/m^3)	Tensile strength (GPa)
Steel fiber	Straight	15	0.12	125	7865	255

Table 3
Concrete mix characteristics (kg/m^3).

Mix	Microsilica	Fly ash	GBFS	Silica sand	Sodium hydroxide	Water	Waterglass	Steel fiber
R-0	46	170	690	900	46	88	316	0
R-1	46	170	690	900	46	88	316	80
R-2	46	170	690	900	46	88	316	155
R-3	46	170	690	900	46	88	316	235
R-4	90	165	650	900	46	88	316	155
R-5	181	146	585	900	46	88	316	155
R-6	272	126	505	900	46	88	316	155

combined in a blender and gradually water was added, followed by the molding of the samples. They were coated and cured at room temperature in the steam curing box at 85 °C for 24 h following molding. They were then removed from the mold and kept in a curing water tank for 28-days before being evaluated.

4. Experimental methods

Several experiments were conducted in this work to determine the mechanical characteristics of steel fiber-reinforced UHP-GPC. The subsequent sections outline the testing procedure.

4.1. Workability

The effect of different fiber inclusions on the workability of fresh ultra-high-performance geopolymer concrete composites was measured in terms of flow diameter as per ASTM C1437–13 [57]. The flow tests were conducted immediately after mixing each batch, and all the mixtures were tested twice.

4.2. Compressive behavior

The compressive behavior of the samples was evaluated in this study using the compressive strength and modulus of elasticity. The compressive strength test was conducted using 100 mm cubic samples per ASTM C39 [58]. Moreover, cylindrical samples of 100 × 300 mm in diameter were utilized to determine the modulus of elasticity per ASTM C-469/C-469M [59]. To accomplish this, a steel ring fitted with a strain gage was placed about the cylindrical sample, the sample's stress-strain measurements were collected, and the modulus of elasticity was calculated as the initial-tangential slope of the stress-strain curve [59].

4.3. Tensile behavior

To determine the splitting tensile strength of the mixtures, the Brazilian test per ASTM C-469 was utilized [60]. To conduct this experiment, 150 × 300 mm cylindrical concrete samples were placed on the lateral surface of a hydraulic jack.

4.4. Flexural behavior

Also, the flexural strength behavior of samples was evaluated in this investigation. A 100 × 100 × 515 mm prism with a center notch was evaluated for this goal using a three-point flexural configuration. The notch is 10 mm in height and 2 mm in width. Three samples of each mixture were prepared and evaluated, and the flexural strength was determined as the mean of the three tested samples.

4.5. Fracture characteristics

Also, the fracture characteristics of samples were investigated in this research. As a result, the fracture energy of the concrete mixes was determined using the equation:

$$G_F = \frac{W_0 + mg\delta}{A_t} \tag{1}$$

where fracture energy, W_0, g, m, A_t, and δ denote the fracture energy, specimen mass, external load work, gravity acceleration, ligament area, and failure deflection, respectively. Moreover, the stress intensity factor (stress intensity factor) is used to determine UHP-GPC fracture resistance [61]. This indicator (stress intensity factor) is related to the efficient crack length and can be computed as follows:

$$a_{eff} = a_0 \frac{C(a_{ef}) f(\frac{a_0}{h})}{C(a_0) f(\frac{a_{ef}}{h})} \tag{2}$$

Where h, a_0, $C(a_0)$, and $C(a_{ef})$ indicate, respectively, the sample's height, the first crack point, the initial crack points flexibility, and any other points in the post-cracking phase. Moreover, $f(a_0/h)$ is the span to depth ratio, and $f(a_{ef}/h)$ can be determined utilizing the equation below:

$$f\left(\frac{a_{ef}}{h}\right) = -2.040\left(\frac{a_{ef}}{h}\right)^3 + 3.870\left(\frac{a_{ef}}{h}\right)^2 - 2.280\left(\frac{a_{ef}}{h}\right) + \frac{0660}{\left(1 + \left(\frac{a_{ef}}{h}\right)\right)^2} \tag{3}$$

Moreover, the stress intensity factor could be computed as follows:

$$K_1 = \sigma(pi * a_{ef} g)^{\frac{1}{2}} \left(\frac{a_{ef}}{h}\right) \tag{4}$$

In which:

$$\sigma = \frac{3FL}{4/2(h - a)^2 b} \tag{5}$$

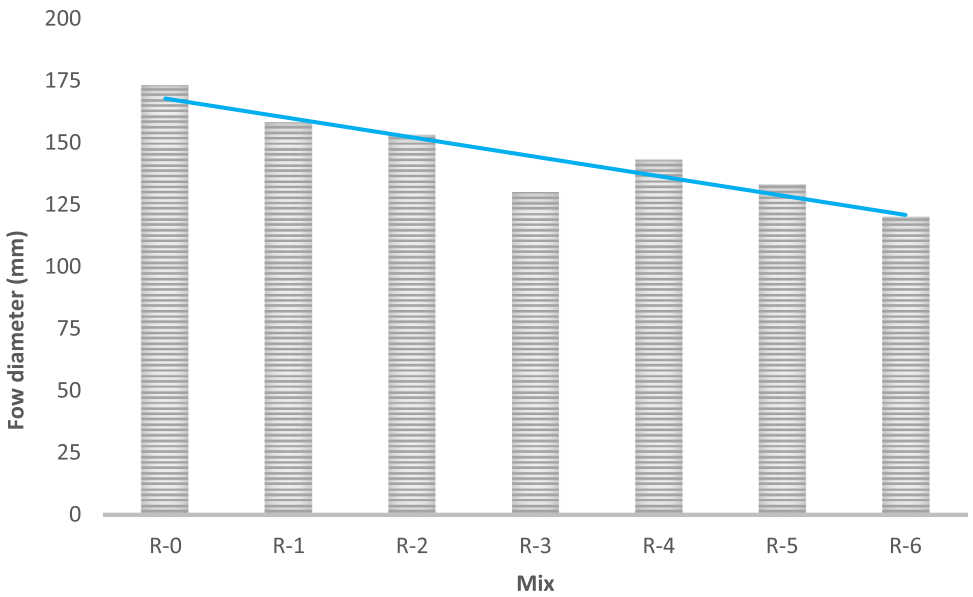

Fig. 2. Effect of different fiber combinations on flowability of the geopolymer composites.

5. Results and discussion

5.1. Workability

The effect of different fiber inclusions on the workability of fresh ultra-high-performance geopolymer concrete composites is compared in Fig. 2. As can be seen, the fresh state properties of geopolymer change significantly with the addition of fibers. It can be established that as the volume fraction of steel fibers increased, the flow diameter decreased respectively. Moreover, it should be noted that the addition of higher volume fraction of steel fibers, such as 2% and 3% produced slightly harsh mixes in the fresh state under the static mode.

Variations in flow diameters, on the other hand, were measured for composites made from ternary mixing of fly ash and slag. The

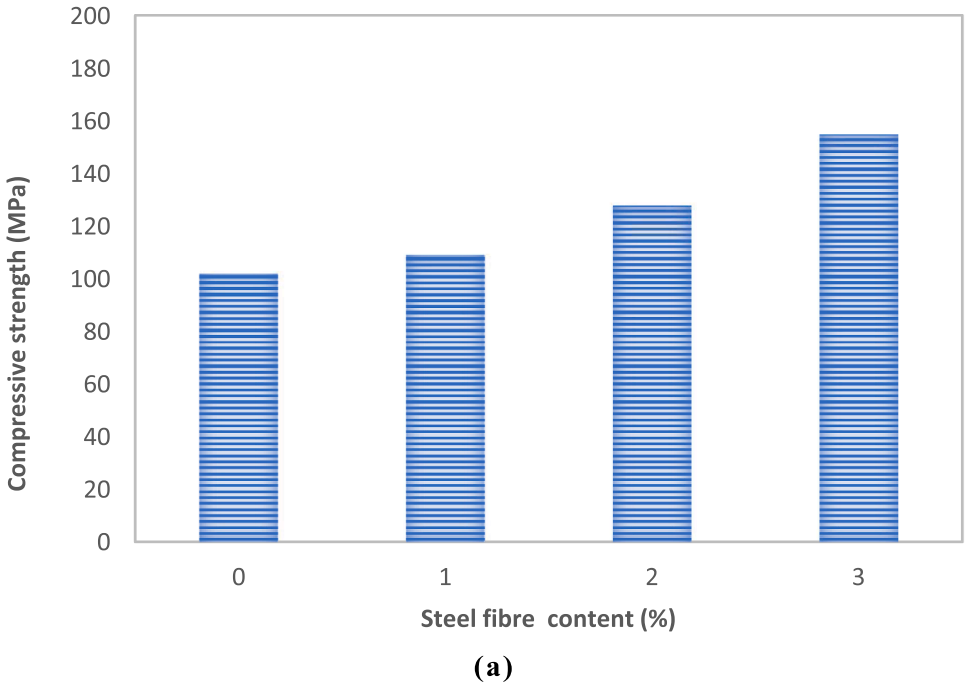

Fig. 3. Influences of steel fiber content on (a) compressive strength; (b) modulus of elasticity of UHP-GPC.

decreased workability of fly ash or slag-containing mixes is due to an increase in calcium content and its quick reactivity with the alkaline activator, where extra calcium functioned as nuclei for the precipitation of dissolved species from fly ash and influenced the coagulation rate.

5.2. Compressive strength, splitting tensile strength, modulus of elasticity

5.2.1. Effects of steel fiber and microsilica contents on compressive strength and modulus of elasticity

Fig. 3 illustrates the correlations between the compressive strength and modulus of elasticity of UHP-GPCs with varying fiber ratios. Both the compressive strength and modulus of elasticity increase as the steel fiber volume increases. Without steel fibers, the average compressive strength and modulus of elasticity are respectively 102 MPa and 27 GPa. When the steel fiber is 1%, the compressive strength and modulus of elasticity are 110 MPa and 28 GPa, respectively. Values raise to 129 MPa and 30 GPa, respectively, when the steel fiber volume is 2%. The maximum compressive strength and modulus of elasticity are achieved with 3% steel fibers, which are 156 MPa and 32 GPa, respectively, 53% and 22% greater than without steel fibers. The pattern in compressive strength and modulus of elasticity variation is similar to past studies on steel fiber-reinforced geopolymer composites [62] and UHPC [63]. Increased steel fiber volume results in a reduction in the average spacing between steel fiber, limiting the onset, and spread of matrix fractures. Moreover, steel fibers with a higher modulus of elasticity help to the improvement of the modulus of elasticity of samples.

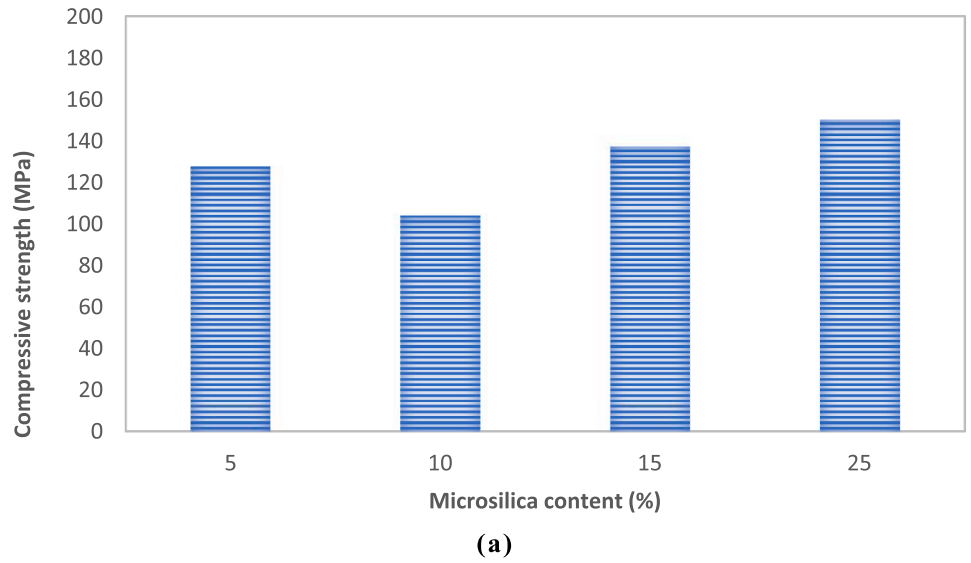

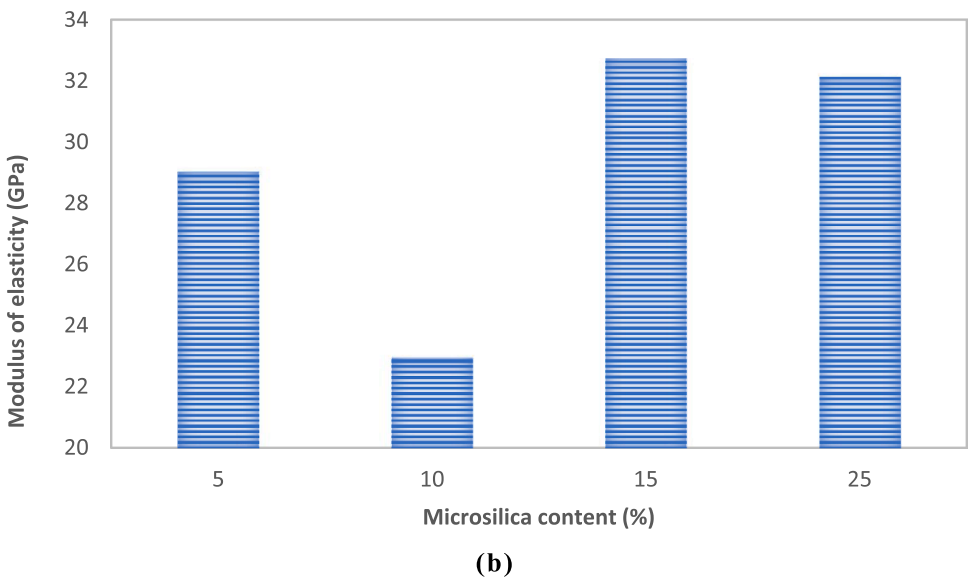

Fig. 4. Influences of microsilica content on (a) compressive strength; (b) modulus of elasticity of UHP-GPC.

The impact of microsilica volume on the compressive strength and modulus of elasticity of UHP-GPC is presented in Fig. 4. The inclusion of microsilica results in a notable change in the compressive strength and modulus of elasticity. The compressive strength and modulus of elasticity are 128 MPa and 30 GPa, respectively, when 5% microsilica is used, but drop by 19% and 22%, respectively, when 10% microsilica is used. Nevertheless, when the microsilica content increased to 15% and 25%, significant improvements in the compressive strengths and modulus of elasticity are noticed. The sample containing 25% microsilica has the maximum compressive strength, while the sample containing 15% microsilica has the maximum modulus of elasticity, which is both greater than the comparable values for the samples containing 3% steel fibers and 10% microsilica. This indicates that by increasing the microsilica volume, the steel fiber volumes may be minimized without impairing the compressive behavior [64,65].

5.2.2. *Effects of steel fiber and microsilica contents on the splitting tensile strength*

The influences of steel fiber and microsilica volume on the splitting tensile strength of UHP-GPC are seen in Fig. 5. As with compressive behavior, increasing steel fiber enhances the splitting tensile strength of UHP-GPC. Strength improves by 15% and 43%, respectively, when the steel fiber volume is increased from 1% to 2% and 3%. Moreover, the splitting tensile strength drops first and subsequently increases when the microsilica volume was increased from 5% to 25%. The lowest splitting tensile strength of 8 MPa is achieved when the microsilica volume is 10%, while the maximum strength of 17 MPa is achieved when the microsilica volume is 25%.

According to a prior study, adding microsilica to steel fiber-reinforced fly ash/GBFS-based geopolymer concrete did not improve the compressive strength but increased the bond strength among the matrix and steel fiber [66]. Nevertheless, given the activity and high effective surface area of microsilica, the dosage of $(SiO_4)^{4-}$ in the solution would substantially enhance upon rapid dissolution of some microsilica, leading to an increase in the existing activator modulus and a decline in activator alkalinity [67], thereby reducing the activation extent of fly ash and GBFS; in contrast, the residual microsilica could optimize the microstructure [25]. When the microsilica volume is increased to 10%, the activator's characteristic changes, altering the generation of reaction products and the development of strength. As the microsilica volume increases to 15% and 25%, the benefit of microstructure improvement outweighs the disadvantage of the activator changes.

5.3. *Flexural behavior*

5.3.1. *Ultimate flexural strength*

Fig. 6 illustrates the ultimate flexural strengths of UHP-GPCs with varying steel fiber and microsilica volumes. The addition of steel fiber improves flexural strength. The ultimate flexural strength increases from 11.5 to 19 MPa with a 1–3% increment in steel fiber. Increased steel fiber amount can increase the contact area between the matrix and steel fiber, hence increasing the ability of the matrix to withstand pressure. Nevertheless, the microsilica volume of UHP-GPC has a significant effect on the ultimate flexural strength. The flexural strength with 10% microsilica was 9% less than the flexural strength with 5% microsilica. The flexural strength increases from 15 to 17 MPa and 22.5 MPa when microsilica is increased continuously from 10% to 15% and 25%. Moreover, samples containing 25% microsilica and 2% steel fibers have greater flexural strength than those containing 3% steel fibers and 10% microsilica. Microsilica's

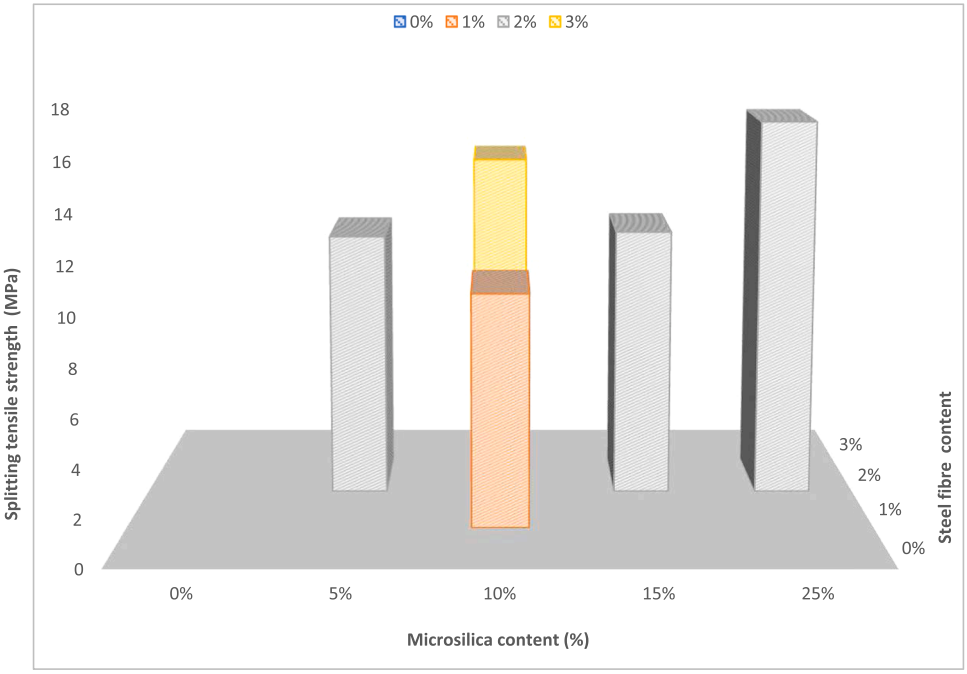

Fig. 5. Influences of steel fiber and microsilica contents on the splitting tensile strength of UHP-GPC.

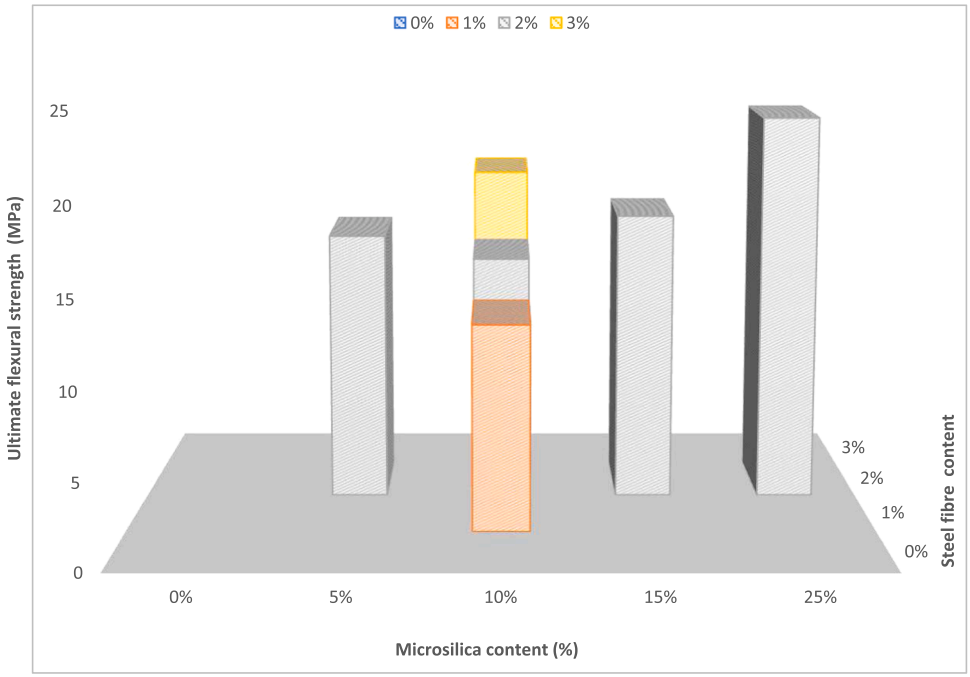

Fig. 6. Ultimate flexural strength of UHP-GPCs with different steel fiber and microsilica contents.

complicated impact is the result of a balance between the influence of the altered activator and the refined microstructure.

5.3.2. *Flexural toughness*

The flexural toughness is calculated as the area under the entire load-deflection curve and ductility is determined from deflection in post-peak region. The flexural behavior of UHP-GPC is illustrated in Table 4. Increased steel fiber content enhances the deflection and strength of the first crack, as well as the peak deflection. When the steel fiber volume is 1%, the deflection and strength of the first crack, as well as the peak deflection, are 0.08 mm, 3.5 MPa, and 0.9 mm, respectively. When the fiber content is 3%, these values increase to 0.09 mm, 6 MPa, and 0.95 mm. According to past studies, the matrix dominates the pre-cracking behavior in UHPC approaches, whereas the first crack behavior is unrelated to the steel fiber volume and form [68]; nonetheless, the contribution of steel fiber is not negligible in this investigation. It may be a result of the geopolymer matrix's extreme brittleness [26]. Moreover, the energy absorbing capability of the samples during the whole cracking process rises as the fiber volume increase. D_{cr}, D_{1f}, and D_{2f} are 1210, 7655, and 32,588 N.mm, respectively, at a 1% fiber volume, and rise to 2100, 11,988, and 51,850 N.mm, respectively, at a 3% steel fiber volume, a 74%, 56%, and 59% increase. This implies that, before cracking, the matrix and steel fibers bear the stress; consequently, the introduction of additional steel fibers increases the stiffness of the samples, thereby increasing their toughness through cracking. In contrast, during the post-cracking process, the fractured part's load is entirely borne by steel fibers; hence, the energy used during UHP-GPC cracking increases according to the amount of steel fiber. Consequently, the flexural toughness of UHP-GPC's is increased.

Table 4 also demonstrates the impact of microsilica on the flexural behavior of UHP-GPC. In comparison to samples containing 5% microsilica, samples containing 10% microsilica exhibit weaker flexural behavior. Nevertheless, increasing the microsilica volume to 15% and 25% improves the flexural behavior of UHP-GPC. Moreover, the introduction of 25% microsilica considerably enhances the toughness during the post-cracking process. According to Table 4, samples with 25% microsilica have the greatest toughness values and equivalent flexural strengths of all samples. For example, the corresponding flexural strengths, $f_{eq1,}$ and f_{eq2}, of samples containing

Table 4
Flexural behavior of UHP-GPC.

Mix	deflection of the first crack (mm)	Strength of the first crack (MPa)	Peak deflection (mm)	D_{cr} (N·mm)	$D_{1\,f}$ (N·mm)	$D_{2\,f}$ (N·mm)	f_{eq1} (MPa)	f_{eq2} (MPa)
R-1	0.07	3.5	0.8	1210	7657	32,588	7.8	6.7
R-2	0.08	4.9	0.8	1635	9735	43,167	9.9	8.8
R-3	0.09	5.9	0.9	2100	11,988	51,756	12.1	10.5
R-4	0.06	4.1	0.6	1310	9446	35,238	9.9	7.1
R-5	0.08	6.5	0.7	2067	11,890	44,288	12.3	9.1
R-6	0.09	6.8	0.9	2295	14,775	68,624	15.1	13.8

25% microsilica are 53% and 60% higher, respectively, than those containing 5% microsilica. As previously stated, the post-cracking behavior is mostly influenced by the bonding between the interface and the steel fiber. The introduction of microsilica alters the bond strength. When the microsilica dose is increased from 10% to 25%, the improved bonding between the matrix and steel fiber results in a decrease in relaxation and an increase in bending behavior [66].

5.4. Fracture characteristics

5.4.1. Fracture energy

The impact of steel fiber amount on the fracture energy of UHP-GPC is seen in Fig. 7. It has been demonstrated that increasing the steel fiber volume results in a considerable increase in fracture energy. The fracture energy value for samples containing 1% steel fibers is 6668 N/m. When fiber intake is increased to 2% and 3%, it increases by 46% and 56.6%, respectively. When the steel fiber amount reaches 2%, the increase in fracture energy appears to be minimal. This is because when the volume increases, the effect of steel fiber becomes restricted due to a reduction in the average area of steel fiber.

Moreover, when the microsilica volume is 10%, the fracture behavior of UHP-GPC is proven to be inferior. Nevertheless, when the microsilica dose is increased to 25%, the fracture energy increases to 14,477 N/m, which is 49.8% and 38.8% greater than that of samples containing 10% microsilica and 2% steel fiber, 3% steel fibers, and 10% microsilica, respectively. This indicates that increasing the microsilica content (over 15%) has a greater effect on improving the fracture resistance of UHP-GPC than increasing the steel fiber amount.

5.5. SEM analysis

Fig. 8 shows the microstructure of UHP-GPC as revealed by scanning electron microscopy. Overall, it was discovered that the mechanical behavior of UHP-GPC was connected to its microstructure. A dense microstructure, in particular, was shown to improve mechanical behavior. Fig. 8-a demonstrate that almost no unreacted substance was detected, indicating that a considerable amount of GGBFS and fly ash were dissolved and then participated in the polymerization.

Meanwhile, the system included globular sodium hydro-aluminosilicate (N-A-S-H), silicates, and aluminates. It should be emphasized that the silicates and aluminates found here included hydro-silicates and hydro-aluminates with a high degree of crystallization, as seen in Fig. 8-b.

Furthermore, the interaction transition zone (ITZ) between the binding phase and aggregate was shown to be significantly denser and less visible. Thus, the significantly greater interfacial transition zone and microstructure as illustrated in Fig. 8-c gave a superior bonding feature with the aggregates, as also found by Xie, Wang, Rao, Wang and Fang [69].

Fig. 8-d depicts the ITZ between steel fiber and UHP-GPC. The ITZ between the UHP-GPC and the steel fiber was nearly faultless, suggesting a superb bonding. It improved the mechanical behavior of UHP-GPC by ensuring the synergy of the steel fiber and matrix.

6. Conclusions

The effects of steel fiber and microsilica on the mechanical characteristics of UHP-GPC were studied and discussed in this article. The following are the major conclusions:

1. The inclusion of steel fibers reduced the workability of fresh ultra-high-performance geopolymer concrete composite mixtures. The workability reduced as the fiber dose increased.
2. The addition of microsilica has a complex effect on the mechanical characteristics of UHP-GPC. Mechanical characteristics were degraded when the microsilica dose was increased from 5% to 15%. However, those characteristics could be regained or further enhanced when the microsilica volume surpassed 15%.
3. When the microsilica volume was greater than 15%, a stronger bonding property between the matrix and steel fiber was noted, resulting in an improvement in the mechanical and fracture characteristics of UHP-GPC. If a sufficient amount of microsilica is utilized, the steel fiber volume can be reduced without impairing the mechanical and fracture characteristics of UHP-GPC.
4. Increased steel fiber volume could enhance UHP-GPC's mechanical and fracture characteristics, such as compressive strength, modulus of elasticity, splitting tensile strength, flexural behavior, fracture energy, and stress intensity factor.
5. According to the SEM examination, the primary reaction products were zeolite, dolomite, C-(N)-AS-H gel, and N-(C)-A-S-H gel. At a microsilica volume of 25%, a substantially adequate polymerization reaction and a densified micromorphology were produced. Meanwhile, SEM investigation revealed the faultless ITZ between G-UHPC and steel fiber.

7. Future studies

In future studies, more detailed investigations need to be conducted on mechanical UHP-GPC, including the effects of curing procedure, binder materials, activator, and fiber type on the performance of mechanical UHP-GPC.

Declaration of Competing Interest

The authors declare that they have no known competing financial interests or personal relationships that could have appeared to

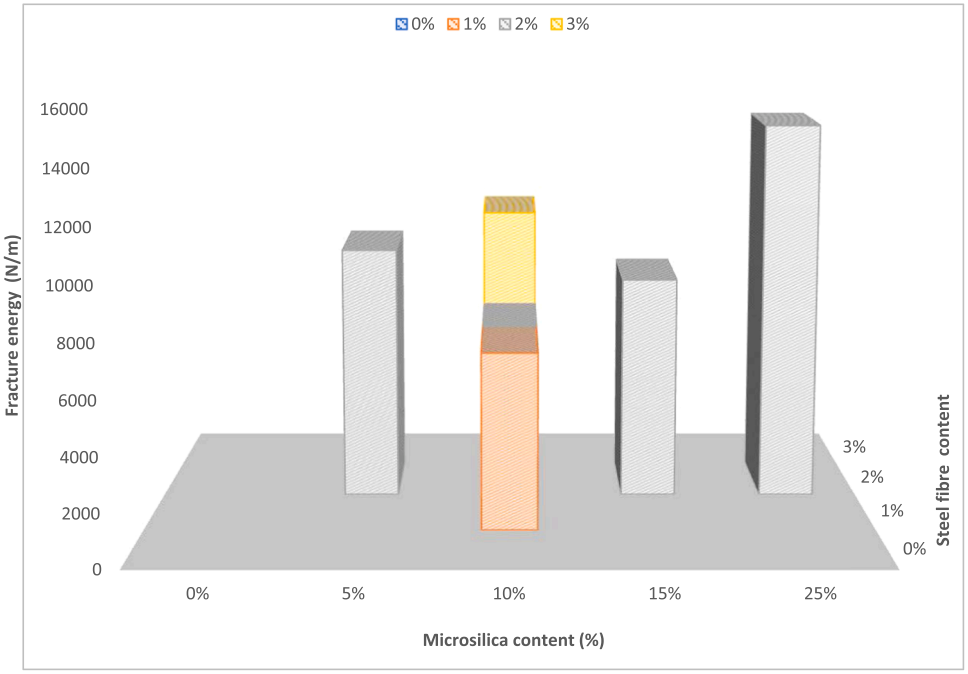

Fig. 7. fracture energy of UHP-GPC with different steel fiber and microsilica contents.

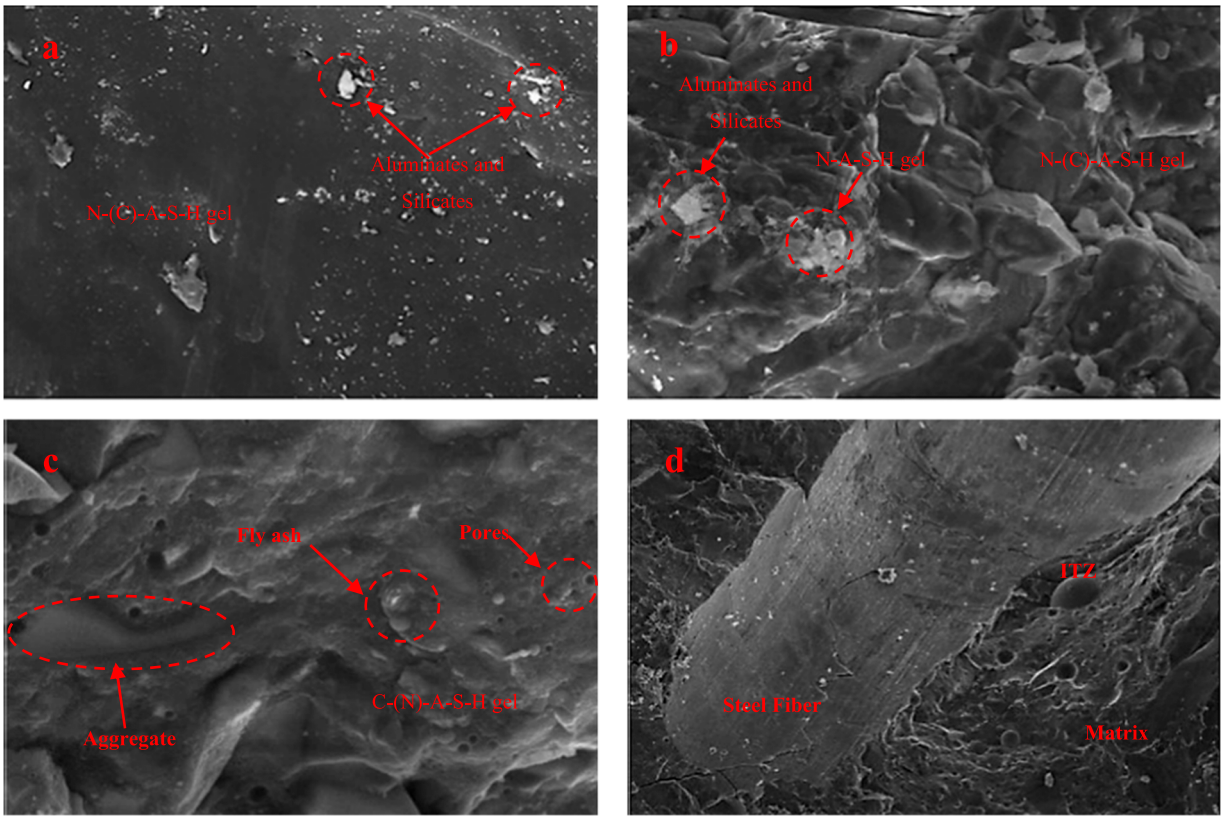

Fig. 8. SEM analysis (10 μm).

influence the work reported in this paper.

Data availability

No data was used for the research described in the article.

References

[1] A. Said, M. Elsayed, A. Abd El-Azim, F. Althoey, B.A. Tayeh, Using ultra-high performance fiber reinforced concrete in improvement shear strength of reinforced concrete beams, Case Stud. Constr. Mater. 16 (2022), e01009.
[2] W. Mansour, M.A. Sakr, A.A. Seleemah, B.A. Tayeh, T.M. Khalifa, Bond behavior between concrete and prefabricated Ultra High-Performance Fiber-Reinforced Concrete (UHPFRC) plates, Struct. Eng. Mech. 81 (3) (2022) 305–316.
[3] L. Ren, Z. Fang, K. Wang, Design and behavior of super-long span cable-stayed bridge with CFRP cables and UHPC members, Compos. Part B Eng. 164 (2019) 72–81.
[4] M. Elsayed, B.A. Tayeh, M. Abou Elmaaty, Y. Aldahshoory, Behaviour of RC columns strengthened with Ultra-High Performance Fiber Reinforced concrete (UHPFRC) under eccentric loading, J. Build. Eng. 47 (2022), 103857.
[5] M. Amin, A.M. Zeyad, B.A. Tayeh, I.S. Agwa, Effect of ferrosilicon and silica fume on mechanical, durability, and microstructure characteristics of ultra high-performance concrete, Constr. Build. Mater. 320 (2022), 126233.
[6] W. Mansour, M. Sakr, A. Seleemah, B.A. Tayeh, T. Khalifa, Development of shear capacity equations for RC beams strengthened with UHPFRC, Comput. Concr. 27 (5) (2021) 473–487.
[7] M. Amin, I.Y. Hakeem, A.M. Zeyad, B.A. Tayeh, A.M. Maglad, I.S. Agwa, Influence of recycled aggregates and carbon nanofibres on properties of ultra-high-performance concrete under elevated temperatures, Case Stud. Constr. Mater. 16 (2022), e01063.
[8] A.S. Faried, S.A. Mostafa, B.A. Tayeh, T.A. Tawfik, The effect of using nano rice husk ash of different burning degrees on ultra-high-performance concrete properties, Constr. Build. Mater. 290 (2021), 123279.
[9] R. Yu, P. Spiesz, H. Brouwers, Development of an eco-friendly Ultra-High Performance Concrete (UHPC) with efficient cement and mineral admixtures uses, Cem. Concr. Compos. 55 (2015) 383–394.
[10] B.A.T. Shaker, M.A. Qaidi, Abdullah M. Zeyad, Afonso R.G. de Azevedo, Hemn Unis Ahmed, Wael Emad, Recycling of mine tailings for the geopolymers production: a systematic review, Case Stud. Constr. Mater. (2022).
[11] B.A.T. Shaker, M.A. Qaidi, Haytham F. Isleem, Afonso R.G. de Azevedo, Hemn Unis Ahmed, Wael Emad, Sustainable utilization of red mud waste (bauxite residue) and slag for the production of geopolymer composites: a review, Case Stud. Constr. Mater. (2022).
[12] A.S. Faried, S.A. Mostafa, B.A. Tayeh, T.A. Tawfik, Mechanical and durability properties of ultra-high performance concrete incorporated with various nano waste materials under different curing conditions, J. Build. Eng. 43 (2021), 102569.
[13] S.M.A. Qaidi, Ultra-high-performance fiber-reinforced concrete: Challenges, 2022.
[14] S.M.A. Qaidi, Ultra-high-performance fiber-reinforced concrete: Applications, 2022.
[15] B.A. Tayeh, A.S. Aadi, N.N. Hilal, B.A. Bakar, M.M. Al-Tayeb, W.N. Mansour, Properties of ultra-high-performance fiber-reinforced concrete (UHPFRC)—A review paper. AIP Conference Proceedings, AIP Publishing LLC, 2019, 020040.
[16] M. Amin, A.M. Zeyad, B.A. Tayeh, I.S. Agwa, Effects of nano cotton stalk and palm leaf ashes on ultrahigh-performance concrete properties incorporating recycled concrete aggregates, Constr. Build. Mater. 302 (2021), 124196.
[17] B.C. Mendes, L.G. Pedroti, C.M.F. Vieira, M. Marvila, A.R. Azevedo, J.M.F. de Carvalho, J.C.L. Ribeiro, Application of eco-friendly alternative activators in alkali-activated materials: a review, J. Build. Eng. 35 (2021), 102010.
[18] W. Mansour, B.A. Tayeh, Shear behaviour of RC beams strengthened by various ultrahigh performance fibre-reinforced concrete systems, Advances in Civil Engineering 2020 (2020).
[19] S.M.A. Qaidi, Ultra-high-performance fiber-reinforced concrete: Cost assessment, 2022.
[20] S.M.A. Qaidi, Ultra-high-performance fiber-reinforced concrete: Durability properties, 2022.
[21] N.K. Baharuddin, F. Mohamed Nazri, B.H. Abu Bakar, S. Beddu, B.A. Tayeh, Potential use of ultra high-performance fibre-reinforced concrete as a repair material for fire-damaged concrete in terms of bond strength, Int. J. Integr. Eng. 12 (9) (2020).
[22] S.M.A. Qaidi, Ultra-high-performance fiber-reinforced concrete: Hardened properties, 2022.
[23] S.M.A. Qaidi, Ultra-high-performance fiber-reinforced concrete: Fresh properties, 2022.
[24] P.S. Ambily, K. Ravisankar, C. Umarani, J.K. Dattatreya, N.R. Iyer, Development of ultra-high-performance geopolymer concrete, Mag. Concr. Res. 66 (2) (2014) 82–89.
[25] A. Wetzel, B. Middendorf, Influence of silica fume on properties of fresh and hardened ultra-high performance concrete based on alkali-activated slag, Cem. Concr. Compos. 100 (2019) 53–59.
[26] S. Aydın, B. Baradan, The effect of fiber properties on high performance alkali-activated slag/silica fume mortars, Compos. Part B Eng. 45 (1) (2013) 63–69.
[27] M. Abdul-Rahman, A.A. Al-Attar, H.M. Hamada, B. Tayeh, Microstructure and structural analysis of polypropylene fibre reinforced reactive powder concrete beams exposed to elevated temperature, J. Build. Eng. 29 (2020), 101167.
[28] S.M.A. Qaidi, Ultra-high-performance fiber-reinforced concrete: Hydration and microstructure, 2022.
[29] S.M.A. Qaidi, Ultra-high-performance fiber-reinforced concrete: Mixture design, 2022.
[30] T. Xie, T. Ozbakkaloglu, Behavior of low-calcium fly and bottom ash-based geopolymer concrete cured at ambient temperature, Ceram. Int. 41 (4) (2015) 5945–5958.
[31] C. Fang, M. Ali, T. Xie, P. Visintin, A.H. Sheikh, The influence of steel fibre properties on the shrinkage of ultra-high performance fibre reinforced concrete, Constr. Build. Mater. 242 (2020), 117993.
[32] L.K. Askar, B.A. Tayeh, B.H. Abu Bakar, A.M. Zeyad, Properties of ultra-high performance fiber concrete (UHPFC) under different curing regimes, Int. J. Civ. Eng. Technol. 8 (4) (2017).
[33] S.M.A. Qaidi, Ultra-high-performance fiber-reinforced concrete: Principles and raw materials, 2022.
[34] A. Mansi, N.H. Sor, N. Hilal, S.M. Qaidi, The impact of nano clay on normal and high-performance concrete characteristics: a review. IOP Conference Series: Earth and Environmental Science, IOP Publishing, 2022, p. 012085.
[35] B.A. Tayeh, B.H. Abu Bakar, M. Megat Johari, A.M. Zeyad, Microstructural analysis of the adhesion mechanism between old concrete substrate and UHPFC, J. Adhes. Sci. Technol. 28 (18) (2014) 1846–1864.
[36] M.M.A.-T. Ibrahim Almeshal, Shaker M.A. Qaidi, B.H. Abu Bakar, Bassam A. Tayeh, Mechanical properties of eco-friendly cements-based glass powder in aggressive medium, Mater. Today. Proc. (2022) (2214–7853).
[37] R.H. Faraj, H.U. Ahmed, S. Rafiq, N.H. Sor, D.F. Ibrahim, S.M.A. Qaidi, Performance of self-compacting mortars modified with nanoparticles: a systematic review and modeling, Clean. Mater. 2772–3976 (2022), 100086.
[38] B.A. Tayeh, B.A. Bakar, M.M. Johari, Y.L. Voo, Evaluation of bond strength between normal concrete substrate and ultra high performance fiber concrete as a repair material, Procedia Eng. 54 (2013) 554–563.
[39] T. Xie, T. Ozbakkaloglu, Influence of coal ash properties on compressive behaviour of FA-and BA-based GPC, Mag. Concr. Res. 67 (24) (2015) 1301–1314.
[40] T. Xie, C. Fang, M.M. Ali, P. Visintin, Characterizations of autogenous and drying shrinkage of ultra-high performance concrete (UHPC): an experimental study, Cem. Concr. Compos. 91 (2018) 156–173.

[41] L.B. de Oliveira, A.R. de Azevedo, M.T. Marvila, E.C. Pereira, R. Fediuk, C.M.F. Vieira, Durability of geopolymers with industrial waste, Case Stud. Constr. Mater. 16 (2022), e00839.
[42] R. Marvila, the Fresh State Properties of Alkali-Activated Mortars by Blast Furnace Slag, Materials.
[43] D.-Y. Yoo, S. Kim, G.-J. Park, J.-J. Park, S.-W. Kim, Effects of fiber shape, aspect ratio, and volume fraction on flexural behavior of ultra-high-performance fiber-reinforced cement composites, Compos. Struct. 174 (2017) 375–388.
[44] S.N. Ahmed, N.H. Sor, M.A. Ahmed, S.M.A. Qaidi, Thermal conductivity and hardened behavior of eco-friendly concrete incorporating waste polypropylene as fine aggregate, Mater. Today Proc., 2022.
[45] H.U. Ahmed, A.S. Mohammed, R.H. Faraj, S.M.A. Qaidi, A.A. Mohammed, Compressive strength of geopolymer concrete modified with nano-silica: experimental and modeling investigations, Case Stud. Constr. Mater. 2 (2022), e01036.
[46] M. Amin, B.A. Tayeh, I.S. Agwa, Effect of using mineral admixtures and ceramic wastes as coarse aggregates on properties of ultrahigh-performance concrete, J. Clean. Prod. 273 (2020), 123073.
[47] S.M.A. Qaidi, Y.Z. Dinkha, J.H. Haido, M.H. Ali, B.A. Tayeh, Engineering properties of sustainable green concrete incorporating eco-friendly aggregate of crumb rubber: a review, J. Clean. Prod. (2021), 129251.
[48] S.M.A. Qaidi, Y.S.S. Al-Kamaki, State-of-the-art review: concrete made of recycled waste PET as fine aggregate, J. Duhok Univ. 23 (2) (2021) 412–429.
[49] A.N. Mohammed, M.A.M. Johari, A.M. Zeyad, B.A. Tayeh, M.O. Yusuf, Improving the engineering and fluid transport properties of ultra-high strength concrete utilizing ultrafine palm oil fuel ash, J. Adv. Concr. Technol. 12 (4) (2014) 127–137.
[50] S.M.A. Qaidi, PET-concrete confinement with CFRP, 2021.
[51] S.M.A. Qaidi, PET-Concrete, 2021.
[52] X. Gao, Q. Yu, H. Brouwers, Characterization of alkali activated slag–fly ash blends containing nano-silica, Constr. Build. Mater. 98 (2015) 397–406.
[53] S.M.A. Qaidi, Behavior of Concrete Made of Recycled PET Waste and Confined with CFRP Fabrics, College of Engineering, University of Duhok,, 2021.
[54] F.A. Jawad Ahmad, Rebeca Martinez-Garcia, Jesús de-Prado-Gil, Shaker M.A. Qaidi, Ameni Brahmia, Effects of waste glass and waste marble on mechanical and durability performance of concrete, Sci. Rep. 11 (1) (2021) 21525.
[55] H.U. Ahmed, A.A. Mohammed, S. Rafiq, A.S. Mohammed, A. Mosavi, N.H. Sor, S.M.A. Qaidi, Compressive strength of sustainable geopolymer concrete composites: a state-of-the-art review, Sustainability 13 (24) (2021) 13502.
[56] R.H. Faraj, H.U. Ahmed, S. Rafiq, N.H. Sor, D.F. Ibrahim, S.M. Qaidi, Cleaner Materials.
[57] C. ASTM, Standard test method for flow of hydraulic cement mortar, C1437 (2007).
[58] A.I.C.Co Concrete, C. Aggregates, Standard Test Method for Compressive Strength of Cylindrical Concrete Specimens, ASTM international, 2014.
[59] A. Standard, Standard Test Method for Static Modulus of Elasticity and Poisson's Ratio of Concrete in Compression, ASTM Stand. C, 2010, p. 469.
[60] A. Standard, C496/c496m (2011) Standard Test Method for Splitting Tensile Strength of Cylindrical Concrete Specimens, Annual Book of ASTM Standards 9 (2004).
[61] M. Lee, B. Barr, Strength and fracture properties of industrially prepared steel fibre reinforced concrete, Cem. Concr. Compos. 25 (3) (2003) 321–332.
[62] X. Guo, X. Pan, Mechanical properties and mechanisms of fiber reinforced fly ash–steel slag based geopolymer mortar, Constr. Build. Mater. 179 (2018) 633–641.
[63] D.-Y. Yoo, J.-H. Lee, Y.-S. Yoon, Effect of fiber content on mechanical and fracture properties of ultra high performance fiber reinforced cementitious composites, Compos. Struct. 106 (2013) 742–753.
[64] A.R. de Azevedo, A.S. Cruz, M.T. Marvila, L.Bd Oliveira, S.N. Monteiro, C.M.F. Vieira, R. Fediuk, R. Timokhin, N. Vatin, M. Daironas, Natural fibers as an alternative to synthetic fibers in reinforcement of geopolymer matrices: a comparative review, Polymers 13 (15) (2021) 2493.
[65] M.T. Marvila, H.A. Rocha, A.R.G. de Azevedo, H.A. Colorado, J.F. Zapata, C.M.F. Vieira, Use of natural vegetable fibers in cementitious composites: Concepts and applications, Innov. Infrastruct. Solut. 6 (3) (2021) 1–24.
[66] M.E. Gülşan, R. Alzeebaree, A.A. Rasheed, A. Niş, A.E. Kurtoğlu, Development of fly ash/slag based self-compacting geopolymer concrete using nano-silica and steel fiber, Constr. Build. Mater. 211 (2019) 271–283.
[67] A.-A. Alyaa A, A. Mazin B, H. Hussein M, T. Bassam A, Investigating the behaviour of hybrid fibre-reinforced reactive powder concrete beams after exposure to elevated temperatures, J. Mater. Res. Technol. 9 (2) (2020).
[68] A.C. 363, Report on High-Strength Concrete (ACI 363R-10), ACI2010.
[69] J. Xie, J. Wang, R. Rao, C. Wang, C. Fang, Effects of combined usage of GGBS and fly ash on workability and mechanical properties of alkali activated geopolymer concrete with recycled aggregate, Compos. Part B Eng. 164 (2019) 179–190.